A Shared Mobility Based Framework for Evacuation Planning and Operations under Forecast Uncertainty

Kati Moug* Huiwen Jia† Siqian Shen‡

Abstract

To meet evacuation needs from carless populations who may require personalized assistance to evacuate safely, we propose a ridesharing-based evacuation program that recruits volunteer drivers before a disaster strikes, and then matches volunteers with evacuees who need assistance once demand is realized. We optimize resource planning and evacuation operations under uncertain spatiotemporal demand, and construct a two-stage stochastic mixed-integer program, first with an expectation-based objective and then a probabilistic constraint, to ensure high demand fulfillment rates. In addition to optimizing the sample average approximations of the two formulations, we study a heuristic approach that is able to provide quick, dynamic and conservative solutions. We demonstrate the performance of our approaches using five test networks of varying sizes based on regions of Charleston County, SC, an area that experienced a mandatory evacuation order during Hurricane Florence. We utilize demographic data and hourly traffic count data from the day of evacuation to estimate the demand distribution. The risk-neutral formulation ensures an average 97% demand fulfillment rate for all test cases and complete fulfillment rates for larger instances at peak-demand time. For smaller instances at off peak time, the risk-averse approach achieves better reliability results.

Keywords: Stochastic programming; evacuation planning; ridesharing; chance-constrained programming

1 Introduction

Planning for evacuations and ensuring efficient operations are key aspects of disaster preparation and mitigation. In the United States, where transportation systems are designed around personal vehicle ownership, evacuation planning for carless populations can be particularly challenging (Urbina and Wolshon, 2003). Further difficulties in evacuation planning arise from the specialized assistance that some carless populations, including people with disabilities and senior citizens, may

*Department of Industrial and Operations Engineering, University of Michigan at Ann Arbor, Email: klmoug@umich.edu;

†Department of Industrial and Operations Engineering, University of Michigan at Ann Arbor, Email: hwjia@umich.edu;

‡Corresponding author; Department of Industrial and Operations Engineering, University of Michigan at Ann Arbor, Email: siqian@umich.edu.

rely on (Renne et al., 2011). To address these issues, we propose a ridesharing program that can be incorporated into a short-notice evacuation plan, recruiting and matching volunteer drivers with evacuees without vehicles, and providing personalized assistance to those who need it. Specifically, we develop models and investigate solution methods for optimal resource planning for setting up the program in the presence of uncertain spatiotemporal demand. Our goal is to determine how many volunteer drivers to recruit before a disaster takes place, so that as many evacuees as possible can be served, when actual demand is uncertain but can be predicted with historical data and behavioral models. We also optimize the operations of such a program, which begin when demand for services is realized and volunteers that were hired must be assigned to riders and routes before the disaster strikes. We assume that the probability distribution of spatiotemporal demand is fully known and obtainable from data, which is then used to sample finite demand samples each with a probability value to build the optimization models. We first formulate this problem as a two-stage stochastic mixed-integer program, with a lexicographical objective to maximize expected number of evacuees served and then minimize expected total distance traveled by all vehicles based on all demand samples. Then, we build a risk-averse counterpart of the risk-neutral stochastic optimization model by using a chance-constrained formulation, to determine how many volunteer drivers to recruit in order to guarantee that we can accommodate all evacuation requests with sufficiently high probability.

1.1 Literature of evacuation planning

Resource planning for shared mobility based evacuation is situated in the field of emergency logistics (Caunhye et al., 2012), and in particular, evacuation planning. Many evacuation planning models are adapted from traffic assignment models and aim to optimize vehicular flow by selecting evacuation routes (Bayram, 2016). A wide variety of papers have taken a multi-objective evolutionary optimization approach (Saadatseresht et al., 2009), a simulation approach (Gan et al., 2016), a deep learning approach (Tanaka et al., 2017), and have utilized a range of heuristic methods (Yusoff et al., 2008) for planning and facilitating evacuation operations. Some of these models incorporate uncertainty, although often in traffic parameters, rather than demand for services, which our models consider. Lim et al. (2019), for example, utilize a distributionally robust chance-constrained formulation to determine evacuation start time and traffic assignment under uncertain traffic demand. Wang et al. (2016) consider an evacuation routing problem under stochastic travel time and a variety of objective functions. For an overview of approaches to optimization of evacuation planning, we direct the reader to Yusoff et al. (2008).

In addition to the study of individual evacuation using personal vehicles, a wide spectrum of previous work has examined bus- or public transportation-based evacuation (see, e.g., Bish, 2011; Kulshrestha et al., 2014; Goerigk et al., 2015), modes that can be effective for transporting large carless populations efficiently to safe zones and minimizing loss of life (Litman, 2006). Because vulnerable populations with specialized needs may not be served well by a fleet of evacuation buses, though, we focus on a smaller-scale ridesharing program, to complement buses in a comprehensive evacuation plan, providing personalized assistance to those who need it.

1.2 Related vehicle routing literature

Our formulation is closely related to and is a stochastic adaptation of the general pickup and delivery problem (GPDP) (Savelsbergh and Sol, 1995), which is a variant of the vehicle routing problem (VRP), aiming to minimize the distance traveled by a fleet of gasoline delivery trucks serving a set of gasoline stations. We refer interested readers to Toth and Vigo (2002) for a comprehensive review of VRP variants and models, as well as optimal/approximate algorithms or meta-heuristics for solving them. While the VRP is often utilized in business applications, such as small package delivery (Wong, 2008), its variants are also used to solve problems of social benefit, including the Dial-a-Ride Problem (Savelsbergh and Sol, 1995; Cordeau and Laporte, 2007) and Senior Transportation Problem (Liu et al., 2018).

In particular, we examine a stochastic VRP variant to increase mobility for underserved populations in response to disaster evacuation orders. Yu and Shen (2020) also examine the transportation needs of underserved populations, under normal, everyday conditions, without a disaster. They study an integrated car-and-ride sharing system, in which drivers without their own vehicles can rent cars from a company at a discounted price, in exchange for providing rides to other users without vehicles who are not able to drive. Their objective is to maximize users served while minimizing expected penalty cost of waiting and overtime, under stochastic travel and service times. In contrast, in the evacuation resource planning problem, we face stochastic demand that will occur randomly in different locations and over time, influenced by the variance in intensity of disasters and the perceived need to evacuate. Thus, the objective in our risk-neutral formulation is to maximize expected evacuees served and minimize expected total distance traveled by all vehicles under forecast uncertainty of potential demand.

1.3 Prior work on evacuation via ridesharing

To the best of our knowledge, this paper is the first to address the resource planning for ridesharing-based evacuation problem, as well as the first to consider uncertainty in the geographical patterns and temporal distribution of demand. On the other hand, the optimization of operations for shared mobility based evacuation has been considered in deterministic settings (Naoum-Sawaya and Yu, 2017; Lu et al., 2020) and under uncertainty in travel time (Li, 2017; Wang, 2020). Naoum-Sawaya and Yu (2017) formulate the ridesharing problem as a mixed-integer program on a network. The spatial distribution of the demand is known, and the objective is to make routing decisions that maximize evacuees served in a fixed time. They also extend their model to minimize evacuation time and to include placement of extra vehicles at pickup nodes for evacuees to drive themselves. Lu et al. (2020) examine ridesharing-based evacuation as a particular instance of the Dial a Ride Problem with Transfers (DARPT). They match drivers and riders using a vehicle-space-time network and a multi-commodity network flow integer program. They test their model using the Chicago traffic network and 10 random locations of drivers and riders. Li (2017) explores ridesharing-based evacuation, using time windows to incorporate a temporal aspect to demand and specifying origins and destinations for both drivers and riders. The author models this problem with an integer

program for matching drivers and riders and providing routing decisions. They also use a robust optimization formulation to incorporate uncertainty in travel time. Both of the deterministic integer program and robust formulation are solved using heuristics.

1.4 Contributions of the paper

We study both risk-neutral and risk-averse formulations and conduct computational tests in five test networks of varying sizes, based on regions of Charleston County, South Carolina, an area that experienced a mandatory hurricane evacuation order in 2018. We estimate the geographical distribution of demand and volunteers available based on granular demographic data and utilize hourly traffic counts over a two-week period that included the evacuation to estimate the temporal distribution of demand.

We plan the total number of volunteer vehicles to recruit, as well as their spatial distribution, in order to either maximize expected evacuees served and minimize total distance traveled by all vehicles (risk-neutral formulation), or ensure complete evacuation with high probability (risk-averse formulation), when facing stochastic spatiotemporal demand. Incorporating stochastic demand requires optimizing over large sets of scenarios, leading to computational challenges in addition to solving the underlying integer program. Modeling realistic instance sizes, with a large number of nodes and arcs that respectively represent locations and their connecting roads in an evacuation network, increases the computational difficulty. We develop algorithms and methods to find near-optimal solutions for this ridesharing-based evacuation problem efficiently.

1.5 Structure of the paper

The remainder of this paper is organized as follows. In Section 2, we describe our mathematical models, beginning with basic assumptions, followed by the two-stage stochastic optimization model, and then the chance-constrained formulation. In Section 3, we describe solution approaches for optimizing different models or deriving near-optimal solutions. In Section 4, we conduct computational studies and test instances of five regional networks based on Charleston County, South Carolina, using traffic data from Hurricane Florence evacuation in September 2018. In Section 5, we summarize the research and discuss future research directions.

2 Mathematical Models

The ridesharing program that we propose has two phases. During the planning phase, volunteers with cars are recruited to provide rides in case of a disaster. Then, when a short-notice evacuation order is given for a particular disaster, such as a hurricane, flood, or slowly-spreading wildfire, individuals who meet eligibility criteria can request rides at a specific location and time. Due to the variability of impact for different disasters, the volume and geographical distribution of demand for evacuation services are not known ahead of time. During the operational phase, once a particular spatiotemporal demand distribution has been realized, decisions are made of where to

route the volunteer drivers, and how many evacuees to load at each location. Emergency drivers are available to assist the volunteer drivers and can be dispatched after we know the realized demand. Because demand for services must be realized in order to optimize corresponding operations, the formulation does not apply to no-notice disasters, such as earthquakes or terrorist attacks.

We begin by defining basic notation, parameters and assumptions in Section 2.1. We then describe the two-stage expectation-based stochastic optimization model in Section 2.2 and the chance-constrained formulation in Section 2.3. For an overview of stochastic programming, which includes two-stage stochastic optimization models and chance-constrained formulations, we direct the interested readers to Birge and Louveaux (2011) and Shapiro et al. (2014).

2.1 Notation, parameters and basic assumptions

We consider a geographical network, denoted $\mathcal{L} = (\mathcal{N}', \mathcal{A}')$, containing locations and connecting roadways in an evacuation region. Specifically, the set of locations is given by $\mathcal{N}' = \mathcal{N}'_P \cup \mathcal{O}' \cup \{h\}$, whose elements are denoted as follows. Evacuees requesting service can arrive at any pickup node $i \in \mathcal{N}'_P$ over a discrete set of time periods $t = 1, \ldots, T$. We have a set of emergency vehicles R and a set of volunteer vehicles S, whose union is defined to be V. Each emergency vehicle $r \in R$, has an origin node $o_r \in \mathcal{O}'$, and each volunteer vehicle $s \in S$ has an origin location $o_s \in \mathcal{O}'$. The location h represents a "safe zone", e.g., the highway. We assume that once a vehicle reaches the safe zone, it has left the evacuation region and is no longer available to pick up additional evacuees. In set $\mathcal{A}'$, there are arcs (o_v, j) for $v \in V = R \cup S$ and $j \in \mathcal{N}'_P$, arcs (i, j) for all $i, j \in \mathcal{N}'_P$ such that $i \neq j$, and arcs (i, h) for all $i \in \mathcal{N}'_P$. Each arc has weights t_{ij}, representing travel time from i to j, and d_{ij}, representing travel distance. If $t_{ij} = d_{ij} = 0$, the physical location of the two nodes is the same (e.g., a volunteer lives in a pickup zone). If $t_{ij} = d_{ij} = \infty$, nodes $i,\ j \in \mathcal{N}'$ are not connected in the evacuation network. Figure 1a depicts one such geographical network with notation illustration, where we exclude arcs $(i, j) \in \mathcal{A}'$ having $t_{ij} = d_{ij} = \infty$.

To construct the corresponding spatiotemporal network $\mathcal{G} = (\mathcal{N}, \mathcal{A})$ based on a given $\mathcal{L}$, we create the set of spatiotemporal nodes $\mathcal{N} = \mathcal{N}_P \cup \mathcal{O} \cup \{h^{T+1}\}$, whose elements we explain as follows. Since evacuees can arrive throughout the planning horizon, we have pickup nodes $\mathcal{N}_P$ of the form i^t, for every $i \in \mathcal{N}'_P$ and $t = 1, \ldots, T$. We assume that all vehicles leave their origin node for a pickup node at time $t = 0$. Thus, we have a set of origin nodes $\mathcal{O} = \{o_v^0 : v \in V = R \cup S\}$. Also, all vehicles need to reach the highway node at time $t = T + 1$, just after the last period that evacuees requesting service can arrive at a pickup location. Thus, the safe zone node in $\mathcal{G}$ is h^{T+1}. (Note that we make these assumptions on the time of the origin nodes and highway node to reduce the size of the network, but it is easy to convert the routing and loading decisions described in later sections to an evacuation plan that includes start times $t = 1, \ldots, T - 1$ for vehicles and times $t = 2, \ldots, T$ to reach the highway.) The set $\mathcal{A}$ of the spatiotemporal network contains idle arcs, connecting (i^t, i^{t+1}), along with travel arcs, $(i^t, j^{t'})$, that exist if the discretized travel time t_{ij} for $(i, j) \in \mathcal{A}'$ is equal to $t' - t$. We also have a set of dummy arcs $(h, o_v^0) \in \mathcal{A}$ for $v \in V$ with travel time and distance 0 to simplify flow balance constraints.

Spatiotemporal demand is a random vector $\mathbf{a}(\tilde{\omega}) = [a_j^t(\tilde{\omega}) :\ j^t \in \mathcal{N}_P]^\mathsf{T} \in \mathbb{Z}_+^{|\mathcal{N}_P| \times T}$ that is a

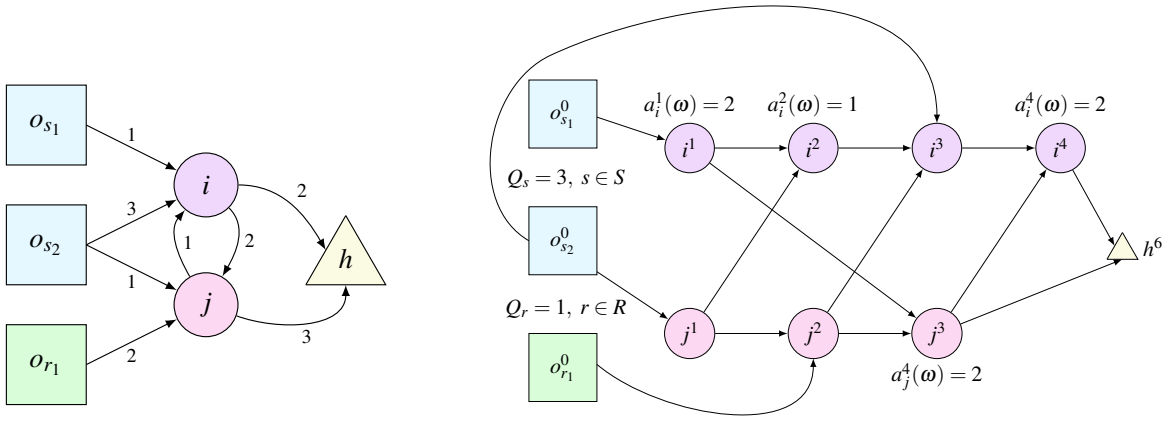

(a) A geographical network with 6 locations, labeled with travel time $t_e,\ \forall e \in \mathcal{A}'$

(b) Corresponding spatiotemporal network given $T = 5$, demand realization $\mathbf{a}(\omega)$ and vehicle capacities $\mathcal{Q}_v$ for $v \in V$

Figure 1: Illustrating the correspondence between a geographical network and a spatiotemporal network given a demand realization and vehicle capacities.

function of random disaster $\tilde{\omega}$, with entries $a^t_j(\tilde{\omega})$ equal to the number of arrivals at each location $j \in \mathcal{N}_P$ and time $t = 1, \ldots, T$, requesting evacuation services. We denote the distribution of $\mathbf{a}(\tilde{\omega})$ as B and the support of $\tilde{\omega}$ as Ω_B. A realization ω of $\tilde{\omega}$ has fixed arrival vector $\mathbf{a}(\omega) \in \mathbb{Z}_+^{|\mathcal{N}_P| \times T}$. Each vehicle $v \in V$ has a maximum capacity $\mathcal{Q}_v$, representing the number of evacuees requesting service that the driver can accommodate in a single ride.

Figure 1 utilizes a small example to illustrate the correspondence between a geographical network and its spatialtemporal transformation, where spatial network $\mathcal{L} = (\mathcal{N}', \mathcal{A}')$ pictured in Figure 1a has $\mathcal{N}'_P = \{i, j\}$, $S = \{s_1, s_2\}$, $R = \{r_1\}$, and arcs labeled by travel time t_e for $e \in \mathcal{A}'$. (We exclude all the arcs e with $t_e = \infty$.) The spatiotemporal network constructed from this spatial network, assuming $T = 5$, is pictured in Figure 1b with description of the capacities of the vehicles, and one realization of demand $\mathbf{a}(\omega)$. One possible evacuation plan for this example is as follows. Volunteer vehicle s_1 travels to i^1 and picks up 2 people, then travels to j^3 and picks up 1 person. Another volunteer vehicle s_2 travels to i^3 and picks up 1 person who has been waiting since $t = 2$. The vehicle waits, traveling along the idle arc to i^4, and picks up 2 more people at i^4. Emergency vehicle r_1 drives to j^2 and waits until $t = 3$ and picks up 1 person at j^3. All three vehicles travel to the highway node h^6, by time $T + 1 = 6$, after picking up their last passengers.

Our objective is to choose which of the available volunteer vehicles $s \in S$ to hire based on one of the following criteria: (i) maximizing expected evacuees served and minimizing expected total distance traveled by all vehicles, or (ii) ensuring that all evacuees are served with high probability. In the next two sections, we describe the models we use based on criteria (i) and (ii), respectively.

2.2 Two-stage stochastic integer program using criterion (i)

To maximize the expected number of evacuees served and minimize expected total distance traveled by all vehicles, we utilize a two-stage stochastic integer program with a risk-neutral expectation-based objective function to evaluate the consequence of planning decisions after realizing values of the uncertain parameter $\mathbf{a}(\tilde{\omega})$. In this model, there is a planning phase and an operational phase. We define planning-phase binary decision variables, $\mathbf{x} = [x_s,\ s \in S]^{\mathsf{T}} \in \{0,1\}^{|S|}$, where $x_s = 1$ if we hire volunteer vehicle $s \in S$, and $x_s = 0$ otherwise. These decisions take place before random disaster $\tilde{\omega}$, with knowledge of the distribution B with support Ω_B of arrival vector $\mathbf{a}(\tilde{\omega})$. After a disaster takes place and realization $\mathbf{a}(\omega)$ is known, the operational phase occurs. At this time, operational decisions are made, with respect to both $\mathbf{x}$ and $\mathbf{a}(\omega)$, with the goal of maximizing evacuees served and minimizing total distance traveled.

In the operational phase, for each scenario $\omega \in \Omega_B$, we define binary variables $\mathbf{z}_\omega = [z_{r\omega},\ r \in R]^{\mathsf{T}} \in \{0,1\}^{|R|}$ to indicate hiring decisions for emergency vehicles $r \in R$, where $z_{r\omega} = 1$ if emergency vehicle r is hired in scenario ω and $z_{r\omega} = 0$ otherwise. For each scenario ω, define binary variables $\mathbf{y}_\omega = [y_{vi^tj^{t'}\omega},\ v \in V,\ (i^t, j^{t'}) \in \mathcal{A}]^{\mathsf{T}} \in \{0,1\}^{|V|\times|\mathcal{A}|}$ to represent routing decisions, where $y_{vi^tj^{t'}\omega} = 1$ if vehicle $v \in V$ travels the arc $(i^t, j^{t'}) \in \mathcal{A}$ in scenario ω and 0 otherwise, along with integer variables $\mathbf{q}_\omega = [q_{vi^t\omega},\ v \in V,\ i^t \in \mathcal{N}_P]^{\mathsf{T}} \in \{0,1\}^{|V|\times|\mathcal{N}_P|}$ that represent loading decisions, where $q_{vi^t\omega}$ is the number of passengers picked up by vehicle $v \in V$ at node $i^t \in \mathcal{N}_P$ in scenario ω. Thus, for each scenario $\omega \in \Omega_B$, given a planning solution $\mathbf{x}$ and demand realization $\mathbf{a}(\omega)$, the corresponding operational phase optimization problem can be modeled as follows:

$$Q(\mathbf{x}, \mathbf{a}(\omega)) = \min_{\mathbf{y}_\omega, \mathbf{z}_\omega, \mathbf{q}_\omega} \quad -\lambda_1 \sum_{v\in V} \sum_{j^t \in \mathcal{N}_P} q_{vj^t\omega} + \lambda_2 \sum_{v\in V} \sum_{(i^t,j^{t'})\in A} y_{vi^tj^{t'}\omega} d_{ij} \tag{1}$$

$$\text{s.t.} \quad \sum_{j^t:(o^0_s,j^t)\in\mathcal{A}} y_{so^0_sj^t\omega} \le x_s,\ s \in S \tag{2}$$

$$\sum_{j^t:(o^0_r,j^t)\in\mathcal{A}} y_{ro^0_rj^t\omega} = z_{r\omega},\ r \in R \tag{3}$$

$$\sum_{i^t:(i^t,j^{t'})\in\mathcal{A}} y_{vi^tj^{t'}\omega} - \sum_{i^t:(j^{t'},i^t)\in\mathcal{A}} y_{vj^{t'}i^t\omega} = 0,\ j^{t'} \in \mathcal{N}, v \in V \tag{4}$$

$$q_{vj^{t'}\omega} \le \mathcal{Q}_v \sum_{i^t:(i^t,j^{t'})\in\mathcal{A}} y_{vi^tj^{t'}\omega},\ j^{t'} \in \mathcal{N}_P, v \in V \tag{5}$$

$$\sum_{j^{t'}\in\mathcal{N}_P} q_{vj^t\omega} \le \mathcal{Q}_v,\ v \in V \tag{6}$$

$$\sum_{v\in V} q_{vj^t\omega} \le \sum_{t=0}^{t'} a^t_j(\omega) - \sum_{v\in V}\sum_{t=0}^{t'-1} q_{vj^t\omega},\ j^{t'} \in \mathcal{N}_P \tag{7}$$

$$\sum_{s\in S} \alpha_s x_s + \sum_{r\in R} \beta_r z_{r\omega} \le C \tag{8}$$

$$\mathbf{z}_\omega \in \{0,1\}^{|R|},\ \ \mathbf{y}_\omega \in \{0,1\}^{|V|\times|\mathcal{A}|},\ \ \mathbf{q}_\omega \in \mathbb{Z}_+^{|V|\times|\mathcal{N}_P|}. \tag{9}$$

In the objective function (1), we maximize the total evacuees served and minimize total distance traveled for all vehicles. Parameters λ_1 and λ_2 determine the weights of the two objectives, with λ_1 assumed to be much larger than λ_2, to heavily preference maximizing evacuees served. Constraints

(2)–(3) ensure that a vehicle v only leaves its origin node o_v^0 if it is hired in that scenario, and constraint (2) ensures that if $x_s = 0$, we cannot dispatch a volunteer's vehicle s from its origin. Constraints (4) are flow balance constraints to ensure that when a vehicle v enters node $j^{t'}$, it also exits that node. Constraints (5) ensure that vehicle v only picks up passengers at node $j^{t'}$ if it drives to node $j^{t'}$. Constraints (6) ensure that no vehicle picks up more passengers than its capacity, $\mathcal{Q}_v$. Constraints (7) ensure that the number of passengers picked up at node j^t by any vehicle is less than or equal to those that have arrived by time t and have not yet been picked up in earlier periods. Constraint (8) is a budget constraint, ensuring that the total cost, calculated based on unit cost α_s of hiring volunteer vehicle $s \in S$ and unit cost β_r of hiring emergency vehicle $r \in R$, is less than or equal to a given budget parameter C.

The overall objective of the two-stage model is to maximize expected evacuees served and minimize expected total distance traveled for all vehicles with respect to the distribution B. We define set X as a deterministic feasible region that encompasses any constraints on the volunteer vehicles hired. For example, in our later computation, X contains upper-bound capacities on the number of volunteers we can hire at each location. One can also include the correlations between the number of volunteers across different locations set X, if such correlations can be obtained a priori and approximated through linear constraints. The function $f(\mathbf{x})$ is a cost function associated with these in-use volunteer vehicles, and $\mathbb{E}_B[\cdot]$ denotes the expectation of $\cdot$ under distribution B of the uncertain parameter. Then the overall problem is given by

$$\begin{aligned} u^* = \min_{\mathbf{x}} \; & f(\mathbf{x}) + \mathbb{E}_B[Q(\mathbf{x}, \mathbf{a}(\tilde{\omega}))] \\ \text{s.t. } & \mathbf{x} \in X \cap \{0,1\}^{|S|}. \end{aligned} \tag{SP}$$

Solving Model (SP) exactly is computationally difficult, even if the support of the distribution is discrete and finite (Kleywegt et al., 2002). Further difficulty arises if the support is continuous, for which (SP) involves multidimensional integration.

Thus, instead we estimate the optimal objective value of (SP) using the Sample Average Approximation (SAA) approach (Kleywegt et al., 2002). In SAA, a Monte Carlo sample Ω of random variable $\tilde{\omega}$ of size N is taken. (Note that Ω is a sample of the random parameter, as opposed to Ω_B, which denotes the support of the distribution.) Because each scenario $\omega \in \Omega$ is independently sampled, we have that $\frac{1}{N}\sum_{n=1}^{N} Q(\mathbf{x}, \mathbf{a}(\omega^n)) \to \mathbb{E}_B[Q(\mathbf{x}, \mathbf{a}(\tilde{\omega}))]$ almost surely as $N \to \infty$. Thus, we have the approximation problem

$$\begin{aligned} \min_{\mathbf{x}} \; & f(\mathbf{x}) + \frac{1}{N}\sum_{n=1}^{N} Q(\mathbf{x}, \mathbf{a}(\omega^n)) \\ \text{s.t. } & \mathbf{x} \in X \cap \{0,1\}^{|S|} \end{aligned} \tag{SP-SAA}$$

Kleywegt et al. (2002) prove a bound for the sample size N required to ensure that the solution to (SP-SAA) is within ϵ of u^* with high probability. The bound is conservative, though, requiring a very large sample size N, which also can be computationally prohibitive.

On the other hand, solving $|\Omega| = N$ subproblems $Q(\mathbf{x}, \mathbf{a}(\omega^n))$ is often much less computationally expensive than minimizing $\frac{1}{N}\sum_{n=1}^{N} Q(\mathbf{x}, \mathbf{a}(\omega^n))$ over the deterministic feasible region. For this reason, we take M Monte Carlo samples of smaller size N, where $\Omega_m = \{\omega_m^1, \ldots, \omega_m^N\}$, to find an optimal solution $\hat{\mathbf{x}}_m$ to (SP-SAA) with objective value $\hat{u}_m$, for $m = 1, \ldots, M$. Let $\overline{u} = \frac{1}{M}\sum_{m=1}^{M} \hat{u}_m$. Mak et al. (1999) showed that $\mathbb{E}[\overline{u}] \leq u^*$, the optimal value for (SP). Thus, we can find an estimated lower bound of the true optimum.

Then, because any candidate solution $\hat{\mathbf{x}}_m$, $m = 1, \ldots, M$ is feasible for any realization of $\tilde{\omega}$ (by letting $\mathbf{q}_\omega = \mathbf{z}_\omega = \mathbf{0}$ in Model (SP) for all scenarios $\omega \in \Omega_B$), we have upper bound $\mathbb{E}_B[Q(\hat{\mathbf{x}}_m, \mathbf{a}(\tilde{\omega}))] \geq u^*$, for each $m = 1, \ldots, M$. Of course, it is difficult to calculate this expectation, as well. Using a sample $\Omega_0 = \{\omega_1^0, \ldots, \omega_{N'}^0\}$ of size $N' > N$ that is independent of the samples $\{\Omega_m\}_{m=1}^M$, we can estimate the expectation with $\frac{1}{N'}\sum_{n=1}^{N'} Q(\hat{\mathbf{x}}_m, \omega_0^n)$. Because this value is an unbiased estimator of $\mathbb{E}_B[Q(\hat{\mathbf{x}}_m, \mathbf{a}(\tilde{\omega}))]$, we have a statistical upper bound $\frac{1}{N'}\sum_{n=1}^{N'} Q(\hat{\mathbf{x}}_m, \mathbf{a}(\omega_0^n)] \geq u^*$. Because this is true for all $\hat{\mathbf{x}}_m$, we can choose the least upper bound, and find the optimality gap between this and $\overline{u}$, to judge the efficacy of the method, which we demonstrate numerically later in Section 4.

2.3 Chance-constrained program based on criterion (ii)

One of the pitfalls of an expectation-based model in a humanitarian setting is its focus on the average performance across all scenarios. Scenarios that deviate from the average may not be served as well by the resource planning solution calculated using the approach in Section 2.2.

To obtain reliable decisions, we consider an alternative chance-constrained formulation (Charnes and Cooper, 1959, 1962), in which we use probabilistic constraints to ensure that a quality of service threshold is met with a particular probability. Luedtke and Ahmed (2008) use SAA to approximate the probability distribution of a chance constraint with a discrete distribution with finite support, which allows the techniques developed in the previously mentioned papers to be utilized for a wider variety of probability distributions. For our problem, chance-constrained models can examine the cost-risk tradeoff of recruiting more volunteer vehicles for disaster evacuation, to find the number of vehicles required to efficiently provide complete evacuation in a range of spatiotemporal demand scenarios, within a specific probability threshold.

Following criterion (ii), we make decisions that satisfy (2)–(9) for all possible realizations of $\tilde{\omega}$, along with the following probabilistic constraint:

$$\mathbb{P}_B\left(\sum_{v\in\mathcal{V}}\sum_{j^t\in\mathcal{N}_P} q_{vj^t\tilde{\omega}} \geq \gamma \sum_{j^t\in\mathcal{N}_P} a_j^t(\tilde{\omega})\right) > 1-\epsilon_0, \tag{CC}$$

which ensures with probability greater than $1-\epsilon_0$ that at least γ proportion of evacuees requesting services are successfully evacuated, with respect to the distribution B of $\mathbf{a}(\tilde{\omega})$. Finding solutions is again computationally difficult, especially if the distribution B is continuous. Following the SAA approach, we approximate the probabilistic constraint (CC) using the empirical distribution of the Monte Carlo sample Ω, which has finite cardinality. We model this empirical probabilistic

constraint using binary decision variables $\mathbf{k} = [k_\omega : \ \omega \in \Omega]^\mathsf{T} \in \{0,1\}^{|\Omega|}$, where $k_\omega = 1$ if the constraint is violated for scenario ω and $k_\omega = 0$ otherwise. Then, we have the following constraints:

$$\sum_{v \in \mathcal{V}} \sum_{j^t \in \mathcal{N}} q_{vj^t\omega} + \mathcal{M}_2 k_\omega \geq \gamma \sum_{j^t \in \mathcal{N}} a_j^t(\omega), \quad \omega \in \Omega, \tag{10}$$

where the constant $\mathcal{M}_2$ in (10) is chosen sufficiently large so that if $k_\omega = 1$ the constraint will be satisfied, and

$$\sum_{\omega \in \Omega} k_\omega \leq \lfloor \epsilon |\Omega| \rfloor, \tag{11}$$

which ensures that the probabilistic constraint is satisfied for a constant $\epsilon \leq \epsilon_0$.

Thus, we formulate the chance-constrained model as a mixed-integer program (MIP) as follows:

$$\min_{\mathbf{x}} \ f(\mathbf{x}) + \frac{1}{N} \sum_{\omega \in \Omega} \sum_{v \in V} \sum_{(i^t, j^{t'}) \in A} y_{vi^tj^{t'}\omega} d_{ij} \tag{CC-SAA}$$

$$\text{s.t.} \ \ (2)\text{–}(9), \forall \omega \in \Omega, \ (10), \ (11).$$

In this model, the objective is to minimize the cost of volunteer vehicles hired, along with the expected distance traveled of all vehicles. Here, we have a probabilistic constraint for the number of evacuees served by the system, the primary objective of the second stage of the expectation-based model. Minimizing distance traveled is a secondary objective, and thus, we do not give it a probabilistic constraint in this model, instead, leaving it in the objective, in order to expand the feasible region and emphasize satisfying the probabilistic constraint for number of evacuees served.

Luedtke and Ahmed (2008) show that feasible solutions to (CC-SAA) satisfy the probabilistic constraint (CC) with probability that goes to 1 as $|\Omega| = N \to \infty$. Again, because the sample size N required to ensure with high confidence that the solutions to (CC-SAA) satisfy (CC) is prohibitively high, we follow a similar method to that described in Section 2.2, of drawing M Monte Carlo samples $\Omega_1, \ldots, \Omega_M$ of size N, and checking if the candidate solutions $\hat{\mathbf{x}}_m$ satisfy $W(\hat{\mathbf{x}}_m, \mathbf{a}(\omega^n)) \geq \gamma \mathbf{a}(\omega^n)$ for scenarios $\{\omega^n\}_{n=1}^{(1-\epsilon_0)\cdot N'}$ of a larger, independent Monte Carlo sample of size $N' > N$, where

$$W(\mathbf{x}, \mathbf{a}(\omega)) = \max_{\mathbf{y}_\omega, \mathbf{z}_\omega, \mathbf{q}_\omega} \ \sum_{v \in V} \sum_{j^t \in \mathcal{N}_P} q_{vj^t\omega}$$

$$\text{s.t.} \ \ (2)\text{–}(9).$$

Here, we check to see if $\sum_{v \in V} \sum_{j^t \in \mathcal{N}_P} q_{vj^t\omega} \geq \gamma \mathbf{a}(\omega)$ for the maximum such value, under the constraints (2)–(9). For the given solution of volunteer vehicles $\mathbf{x}$, the constraint (CC) is satisfied if and only if $W(\hat{\mathbf{x}}_m, \mathbf{a}(\omega^n)) \geq \gamma \mathbf{a}(\omega^n)$ for $(1-\epsilon_0) \cdot N'$ scenarios $\{\omega^n\}_{n=1}^{(1-\epsilon_0)\cdot N'}$. We demonstrate the computational efficacy of the SAA-based chance-constrained model later in Section 4.5

3 Solution Algorithm

We demonstrate the computational performance of directly solving (SP-SAA) and (CC-SAA) using off-the-shelf optimization solvers in Section 4, showing that reliable solutions can be found within an hour for test instances with up to 16 locations and 4 time periods, with $|\Omega_m| = 100$ for a relaxation of (SP-SAA) and $|\Omega_m| = 25$ or 50 for (CC-SAA), for samples $m = 1, \ldots, M$. On the other hand, in this problem, volunteer drivers are low-cost and fairly easy to recruit, which implies quick, conservative solutions could also provide useful information to decision makers. For larger problem sizes that cannot be accommodated by (SP-SAA) or (CC-SAA), heuristic-based approaches can be especially helpful for improving evacuation efficiency and also planning under uncertainty.

For this reason, we develop an algorithm that constructs a single deterministic worst-case scenario from all scenarios in a Monte Carlo sample Ω_m to find a feasible solution $\hat{\mathbf{x}}_m$ to (SP-SAA), $m = 1, \ldots, M$. Later, we measure the performance of this approach using second-stage function $Q(\hat{\mathbf{x}}_m, \mathbf{a}(\omega))$, described in Section 2.2, checking the total distance traveled and evacuees served, and whether inequality $\sum_{v \in \mathcal{V}} \sum_{j^t \in \mathcal{N}} q_{vj^t\omega} \geq \gamma \sum_{j^t \in \mathcal{N}} a^t_j(\omega)$ is satisfied, for each scenario $\omega \in \Omega_0$, an independent Monte Carlo sample of size $N' > N = |\Omega_m|$. In this way, we can compare the performance of the mean distance traveled and mean evacuees served for the (SP-SAA)-feasible solution $\hat{\mathbf{x}}_m$ given by the algorithm, while checking to see if (CC) is satisfied by the risk-neutral formulation. Because we use $Q(\hat{\mathbf{x}}_m, \mathbf{a}(\omega))$ to compare candidate solutions $\hat{\mathbf{x}}_m$, for $m = 1, \ldots, 5$, the best candidate solution is the one that minimizes the objective of (SP-SAA).

The nature of ridesharing suggests that many practical applications of these models would have a particular network structure. Because the pickup nodes $\mathcal{N}'_P$ in the spatial network $\mathcal{L}$ represent zones of the planning region, it is likely that there is overlap in the physical locations represented by a pickup node and a vehicle origin node. Volunteers in the ridesharing program will likely be recruited from the community evacuating, and emergency vehicles will likely be located within the community as well. Thus, one mild assumption that we can apply is that each vehicle $v \in V$ has an origin node o_v such that distance $d_{o_v i} = 0$ for exactly one $i \in \mathcal{N}'_P$. We say vehicle v *originates* in zone i, and denote the set of volunteer vehicles that originate in zone i as S_i.

Under this assumption, we provide the details of a greedy heuristic in Algorithm 1 as follows. It constructs a worst-case spatial scenario ω_{spatial} from a Monte Carlo sample Ω_m of random variable $\tilde{\omega}$, defining spatial demand at location $i \in \mathcal{N}'_P$ in ω_{spatial} to be $a^i_{\max}$, the largest total number of evacuees that arrive at location i over all scenarios $\omega \in \Omega_m$. Then, we find a set of vehicles with the capacity to accommodate all demand in ω_{spatial}. For simplicity of language, for the remainder of Section 3, "demand" and "evacuees" refer to the demand in this worst-case scenario.

We assume that in the worst-case scenario, the emergency vehicles will be filled to their full capacity. For this reason, the overall goal of Algorithm 1 is to hire enough volunteer vehicles to satisfy the difference between the demand and the total capacity for all emergency vehicles. The algorithm first matches demand and volunteer vehicles located at the same node $i \in \mathcal{N}'_P$, hiring and completely filling volunteer vehicles $s \in S_i$ one at a time, in order from the largest to the smallest

vehicle capacity $\mathcal{Q}_s$ for $s \in S_i$. It continues to hire volunteer vehicles and fill them with demand at node $i \in \mathcal{N}'_P$ until the location runs out of volunteer vehicles or people who need rides, or until a global condition is met, i.e., the remaining unassigned demand from all locations is less than or equal to total capacity of the emergency vehicles.

To do this, a set of empty volunteer vehicles, E_i, is initialized as S_i. Each volunteer vehicle s has a remaining capacity variable $\mathcal{Q}_s^{\text{rem}}$, which is initialized as its capacity $\mathcal{Q}_s$. When a volunteer vehicle $s \in E_i$ is hired, it is removed from E_i and added to set S_H. Once the vehicle is hired, it is filled to capacity, or with remaining unassigned individuals at the node, whichever is smaller. At this point, we simultaneously decrease $\mathcal{Q}_s^{\text{rem}}$ and a_{rem}^i, a variable which represents remaining unassigned demand at location $i \in \mathcal{N}'_P$, accordingly.

Once we have matched as many people and seats as possible at each location $i \in \mathcal{N}'_P$, we test to see if the total remaining demand for all locations $i \in \mathcal{N}'_P$, denoted a_{rem}, exceeds the total capacity for all emergency vehicles $r \in R$. If so, we stop. Otherwise, we continue to fill and hire volunteer vehicles until remaining demand a_{rem} falls to the level of the total capacity of the emergency vehicles or we run out of empty volunteer vehicles in $\bigcup_{i \in \mathcal{N}'_P} E_i$ and remaining capacity in hired vehicles.

To do this, Algorithm 1 repeatedly chooses the pickup location i^* with the greatest remaining demand, $i^* = \arg\max_{i \in \mathcal{N}'_P} a_{\text{rem}}^i$. If there is a volunteer vehicle s in the set of hired cars S_H such that remaining capacity $\mathcal{Q}_s^{\text{rem}} > 0$, the algorithm identifies the closest such vehicle to i^*, and fills the vehicle as much as possible. Otherwise, the closest empty volunteer vehicle, in the set $E_j \subseteq \bigcup_{i \in \mathcal{N}'_P} E_i$, to i^* is added to S_H and removed from E_j, and filled as much as possible.

In Step 1, we construct a worst case spatial demand scenario, by examining total demand over periods $1, \ldots, T$ at pickup location $i \in \mathcal{N}'_P$ and maximizing this value over all scenarios $\omega \in \Omega_m$. The sample size $|\Omega_m|$ only affects this first step – thus, Algorithm 1 can be used with large Monte Carlo samples.

We initialize a set of variables in Steps 2–3. The cars that have been assigned at least one evacuee are contained in the set S_H, and thus, S_H is empty at first. Steps 4–14 hire the initial set of volunteer vehicles, matching demand and vehicles by location. Step 5 initializes a set of cars that have not yet been assigned evacuees, E_i, as S_i, the set of volunteer vehicles that originate at i. Then the condition in Step 6 checks to see if the total remaining demand is greater than the sum of the capacities of the emergency vehicles and the remaining capacity of the volunteer vehicles that have already been hired. The while loop also checks to see if there is still remaining demand in the location and cars to be hired in the location. If these conditions are met, in Step 7, we hire the volunteer vehicle at location i with greatest capacity. Then, in Step 8, we check to see if demand left at the location is at least as large as the capacity of the volunteer vehicle we have hired. In this case, in Step 9, we fill the volunteer vehicle and decrease the remaining demand. Otherwise, remaining capacity in the volunteer vehicle exceeds demand and we have seats left in the vehicle, as seen in Step 11. The for loop can be executed in a particular order based on the specifics of the instance. For example, if a network has a single emergency origin location, pickup nodes can be chosen in order from furthest to closest to the emergency origin node, so that if the total remaining demand condition in Step 6 is met quickly, the areas furthest from the emergency vehicles will be

Algorithm 1 A greedy-based heuristic for obtaining shared-mobility-based evacuation plans.

Define $a^i_{\max} := \max_{\omega \in \Omega_m} \{\sum_{t=1}^{T} a^t_i(\omega)\}$, $\forall\ i \in \mathcal{N}'_P$.
Initialize $a^i_{\text{rem}} := a^i_{\max}$, $\forall\ i \in \mathcal{N}'_P$, and $a_{\text{rem}} := \sum_{i \in \mathcal{N}'_P} a^i_{\text{rem}}$.
Initialize $S_H := \varnothing$ and $\mathcal{Q}^{\text{rem}}_s := \mathcal{Q}_s$, $\forall\ s \in V$.
for $i \in \mathcal{N}'_P$ **do**
    Initialize $E_i := S_i$.
    while $a_{\text{rem}} - \sum_{s \in S_H} \mathcal{Q}^{\text{rem}}_s > \sum_{r \in R} \mathcal{Q}_r$ **and** $a^i_{\text{rem}} > 0$ **and** $|E_i| > 0$ **do**
        Choose $s \in E_i$ with maximum $\mathcal{Q}^{\text{rem}}_s$. Add s to S_H and delete s from E_i.
        if $\mathcal{Q}^{\text{rem}}_s \leq a^i_{\text{rem}}$ **then**
            Update $\mathcal{Q}^{\text{rem}}_s := 0$, $a^i_{\text{rem}} := a^i_{\text{rem}} - \mathcal{Q}^{\text{rem}}_s$, and $a_{\text{rem}} := a_{\text{rem}} - \mathcal{Q}^{\text{rem}}_s$.
        else
            Update $\mathcal{Q}^{\text{rem}}_s := \mathcal{Q}^{\text{rem}}_s - a^i_{\text{rem}}$, $a^i_{\text{rem}} := 0$, and $a_{\text{rem}} := a_{\text{rem}} - a^i_{\text{rem}}$.
        end if
    end while
end for
while $a_{\text{rem}} - \sum_{s \in S_H} \mathcal{Q}^{\text{rem}}_s > \sum_{r \in R} \mathcal{Q}_r$ **and** $(\sum_{i \in \mathcal{N}'_P} |E_i| > 0$ **or** $\sum_{s \in S_H} \mathcal{Q}^{\text{rem}}_s > 0)$ **do**
    Choose pickup location i^* with greatest remaining demand $a^{i^*}_{\text{rem}}$, over nodes in $\mathcal{N}'_P$.
    if $\sum_{s \in S_H} \mathcal{Q}^{\text{rem}}_s > 0$ **then**
        Find node $i \in \mathcal{N}'_P$ closest to i^* such that $\mathcal{Q}^{\text{rem}}_s > 0$ for $s \in S_i$. Repeat Steps 8-12.
    else
        Find node $i \in \mathcal{N}'_P$ closest to i^* such that $|E_i| > 0$. Repeat Steps 7-12.
    end if
end while
return S_H.

assigned volunteer drivers.

Then, Steps 15–22 fill all remaining capacity in the hired cars, and add more cars if necessary. The loop runs as long as total remaining demand exceeds the total emergency car capacity and either some car has not been hired or some capacity remains in a hired car. In Step 16, we choose the location with the most demand that has not yet been assigned a volunteer vehicle. Then, Step 17 checks to see if any of the hired volunteer vehicles are partially full. If so, in Step 18, demand at location i^* is fulfilled by the closest volunteer vehicle. Note that there is at most one hired volunteer vehicle s at location i such that $\mathcal{Q}_s^{\text{rem}} > 0$ at any given time. If all hired cars are full, the closest available car to location i^* is hired and filled in Step 20.

4 Computational Studies

To test the efficacy of our models and Algorithm 1, we study a number of test cases based on the greater Charleston area, a region located on the Atlantic coast that experienced a mandatory evacuation order in 2018 for Hurricane Florence (see Manno, 2018). We begin by discussing the generation of demand scenarios to form samples needed by the SAA approach in Section 4.1. We describe parameter settings in Section 4.2 and experimental design and computer characteristics in Section 4.3. Then, we discuss benchmark tests of solving the expectation-based stochastic optimization model in Section 4.4, followed by tests and results of the chance-constrained programming formulation and Algorithm 1 in Section 4.5.

4.1 Scenario generation method overview

In the literature, random evacuation scenarios are generated in a variety of ways. Legg et al. (2010) represent regional hurricane hazard in North Carolina with a set of 100 hurricane scenarios (with 33 involving evacuation) constructed using HAZUS-MH probabilistic analysis (FEMA, 2006). Li et al. (2012) use these 33 scenarios to study a shelter location model in North Carolina, using estimates of geographical distribution and volume of evacuees and individuals requiring shelter determined by HAZUS-MH software. They also describe temporal distribution of evacuation using the Rayleigh distribution, which was used by Tweedie et al. (1986) to describe estimates for evacuation times given by Oklahoma Civil Defense Office experts. Ben-Tal et al. (2011), who study a dynamic traffic assignment problem in emergency evacution, assume the temporal distribution of evacuation is an S-shaped curve and utilize a mathematical formulation given by Radwan et al. (1985).

To generate demand scenarios in different samples, we construct a set of five evacuation networks, based on Charleston County, South Carolina. We use hourly traffic counts from a continuous count station on highway I-26 in Charleston on the day the 2018 Hurricane Florence evacuation order took effect, to estimate of the temporal distribution of demand. Because the populations who can request service from our program are distinct from populations who are most likely to provide service, we use census data on the demographics of tracts in Charleston County to estimate the geographical distribution of both evacuees requesting service and volunteers available.

4.2 Parameter settings

4.2.1 Building spatiotemporal networks

To construct a spatial network, census tracts in Charleston County are aggregated to obtain 48 spatial zones – each represented as a node in the network. Distances and travel times between nodes are determined using the centers of the spatial zones. The coordinates of each geographic center are first found using ArcGIS Pro, and then utilized in Google Distance API to determine d_{ij} and t_{ij} for each $i,\ j \in \mathcal{N}'$. This spatial network is separated into five subnetworks, ranging in node size from 4 to 16, based on natural geographical boundaries, as depicted in Figure 2a.

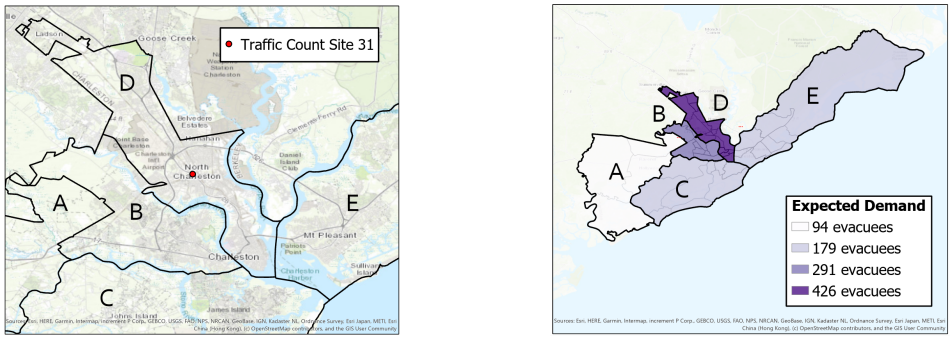

(a) Location of traffic count Site 31 and demarcation of regions in Charleston County.

(b) Total expected demand for ridesharing services in each region.

Figure 2: Illustration of regions and demand hot zones in Charleston County.

Temporal evacuation patterns are estimated using hourly traffic count data from Site 31, a Continuous Count Station on Highway I-26 in Charleston, on September 11, 2018, from 6:01 am-1:00 pm (South Carolina Department of Transportation, 2018). The location of Site 31 also can be seen in Figure 2a. The governor of South Carolina had issued a mandatory evacuation order for coastal areas by noon of that day (Manno, 2018). This seven-hour time horizon is divided into 28 periods of 15 minutes each. Because travel time t_{ij} is measured in seconds, the length of an interval $(t, t+1)$ for $t = 1, \ldots, 27$ is 900.

A spatiotemporal network $(\mathcal{N}, \mathcal{A})$ is constructed from each regional subnetwork $(\mathcal{N}', \mathcal{A}')$, with origin node o_i^0 for each spatial zone $i \in \mathcal{N}'$ and origin node o_{j*}^0 for a centrally located spatial zone. Here, we assume that for each volunteer s, we have $o_s^0 := o_i^0$, the zone i where the volunteer lives. For each emergency vehicle r, we have $o_r^0 := o_{j*}^0$, a depot where all emergency vehicles originate. In this way, regardless of the number of vehicles utilized in a particular test, the structure of the spatiotemporal network remains the same. In addition to origin nodes, the spatiotemporal network includes pickup nodes i^t for $i \in \mathcal{N}'$, $t = 1, \ldots, T$ and highway node h^{T+1}. An arc is drawn from i^t to $j^{t'}$ if $t' - t = \left\lceil \frac{t_{ij}}{900} \right\rceil$. For every spatial zone, a state-determined evacuation route run through either the zone or an adjacent zone. Thus, the highway is reachable in one period for every pickup node.

4.2.2 Demand generation and samples

Demand at each spatiotemporal node is assumed to be Normally distributed with mean $\mu_{i,t}$ and variance $\sigma^2_{i,t}$, independent of demand at other times or locations. The mean $\mu_{i,t}$ is determined by first estimating total demand at location $i \in \mathcal{N}'_P$ over all periods, denoted μ_i, using data on the median income and number of elderly people living in census tracts located in each node (United States Census Bureau, 2018a,b). The mean value of elderly people (65+) assumed to take advantage of our service is determined by taking a percentage of the total elderly population in that census tract. The percentage is determined by the quartile of the median income for people 65 years and older in that census tract, as seen in Table 1. Here, median income serves as a proxy for vehicle ownership. We then determine μ_i for each zone i by adding the mean value for each tract in the aggregated zone i, and round to the nearest integer. In the Appendix, we visualize the spatial distribution of μ_i, $i \in \mathcal{N}'$ for each of the five regions in Figures 7a, 7c, 8a, 8c, and 9a.

Table 1: Percentage of 65+ population requesting ridesharing-based evacuation service in census tract

Quartile	Median Income Range	Percentage
1	[$16,726, $34.235.50]	5%
2	($34.235.50, $45,600]	2.5%
3	($45,600, $62,106.50]	1.25%
4	($62,106.50, $146,477]	.625%

We assume that the same temporal evacuation pattern holds for each location. Using the aforementioned traffic count data, we estimate the percentage of overall evacuees who leave in hour h, denoted p_h, where $\sum_{h=1}^{7} p_h = 1$. Site 31 is chosen because the traffic count pattern clearly changed the day of the evacuation deadline. Figure 3 shows the similar traffic patterns present on normal work days – Tuesday, September 4 to Friday, September 7, along with Monday, September 10 – and present on weekend/holiday days – the Saturdays, Sundays, and Labor Day Monday. Then, a markedly different pattern appears Tuesday, September 11. Residents were ordered to evacuate by noon that day (Manno, 2018).

Figure 3: Hourly traffic counts for September 1 to September 13, 2018 on Highway I-26 in Charleston County.

In addition, the data shows a clear pattern of greater westbound traffic the day of the evacuation

deadline, in the direction away from the coast, which suggests that many of those passing by this traffic count site were evacuees. While the ratio of total westbound to total eastbound traffic on Tuesday, September 4 is .98, meaning traffic is roughly evenly split by east/west, the ratio for westbound to eastbound traffic on Tuesday, September 11 is 2.33.

There is an overall reduction in traffic from September 4 to September 11 with about 20% of the total eastbound traffic and about 50% of the total westbound traffic. Because those traveling in the eastern direction are most likely not immediately evacuating, we use these travelers as a proxy for the proportion of people in the westbound direction who are not evacuees.

For each hour h, we calculate the number of evacuees with the following formula:

$$W_{11}^h - W_4^h \times \frac{E_{11}^h}{E_4^h},$$

where W_{11}^h (or E_{11}^h) represents the westbound (or eastbound, respectively) traffic count at hour h on September 11, 2018, and W_4^h (or E_4^h) represents the westbound (or eastbound, respectively) traffic count at hour h on September 4, 2018, a normal workday. Here, W_4^h estimates the number of westbound commuters on a normal Tuesday, and $\frac{E_{11}^h}{E_4^h}$ estimates the proportion of Tuesday westbound commuters who went to work the morning of September 11, 2018 rather than evacuating at that time. The idea is that the eastbound and westbound directions each have regular morning commuters (i.e., two distinct groups that travel in the same direction in the morning and at night). We assume these groups are similar in their evacuation timing decisions. Thus, the proportion of westbound travelers who have decided not to evacuate and are carrying about their normal business on September 11, 2018 should be a similar proportion to the eastbound travelers, all of whom we assume are not evacuating, since they travel toward the coast.

The hours of 6:01 am to 1 pm are found to have the highest volume of evacuees. The percentage of evacuees in each hour of the roughly 2,300 estimated evacuees over the 7-hour period is used to estimate p_h. The parameters p_h that we use are presented in Table 2. For period t in hour h, the mean $\mu_{i,t}$ is determined by multiplying $\frac{p_h}{4}\mu_i$. The variance $\sigma_{i,t}^2$ is assumed to be $.3\mu_{i,t}$.

Table 2: Temporal distribution of evacuees at Site 31 during different hours on September 11, 2018.

Hour	Percentage of Evacuees
6:01-7:00 am	12%
7:01-8:00 am	18%
8:01-9:00 am	14.5%
9:01-10:00 am	14.5%
10:01-11:00 am	15.5%
11:01 am-12:00 pm	13%
12:01-1:00 pm	12.5%

We further use a rolling horizon approach, performing all the tests for each hour separately. Since Hours 3 and 4 have the same demand distributions, we test Hours 1, 2, 3, 5, 6, and 7, with $T = 4$. For each region and hour, we perform Monte Carlo sampling, generating 5 samples of 100 scenarios each following the aforementioned distribution. Denote these samples $\Omega_m^{\mathcal{N}'h}$, $m = 1, \ldots, 5$. For each scenario $\omega \in \Omega_m^{\mathcal{N}'h}$ and spatiotemporal node $i^t \in \mathcal{N}_P$, the number of arrivals is $a_i^t(\omega) =$

$\max\{[X_{i,t}], 0\}$, where $X_{i,t}$ is a random variable with distribution $N(\mu_{i,t}, \sigma^2_{i,t})$. An independent sample $\Omega^{\mathcal{N}'h}$ of 1000 scenarios is generated in the same manner for out-of-sample testing. For ease of notation, we denote the total expected demand over an hour h in all zones in network $\mathcal{N}'$ as $\mu_h^{\mathcal{N}'}$, where $\mu_h^{\mathcal{N}'} = \sum_{i\in\mathcal{N}'} \sum_{t=4(h-1)+1}^{4h} \mu_{i,t}$.

We assume that about 60% of demand will be satisfied by volunteer cars, and 40% by emergency cars. To determine the number of vehicles available in hour h, we use the following formula: $|S| = .6 \times \sum_{i\in\mathcal{N}'} \sum_{t=4(h-1)+1}^{4h} \frac{\mu_{i,t}}{\mathcal{Q}_s} \times 2$ and $|R| = .4 \times \sum_{i\in\mathcal{N}'} \sum_{t=4(h-1)+1}^{4h} \frac{\mu_{i,t}}{\mathcal{Q}_r} \times 2$. Here, $\mathcal{Q}_v$ is fixed for $v \in R$ and $v \in S$, and 2 is a factor to increase the likelihood that the pool of available cars can handle demand scenarios that arise. The capacities used for this study are $\mathcal{Q}_s = 3$ and $\mathcal{Q}_r = 7$.

4.2.3 Settings of supply (volunteers)

The spatial distribution of volunteer cars is estimated using data on the population size of individuals ages 25-64 and median income in the census tracts at particular nodes (United States Census Bureau, 2018a,b). Higher median income in a particular census tract is assumed to increase likelihood of vehicle ownership, and thus, ability to act as a volunteer driver. Each origin node, at location i, is assigned an estimated proportion of volunteer drivers, v_i. The number of volunteer cars at an origin node at location i is determined by calculating $[v_i \cdot |S|]$, the nearest integer. Any vehicles not assigned by this process are randomly assigned to an origin node. The spatial distribution of volunteers on average can be seen for each of the five networks in Figures 7b, 7d, 8b, 8d, and 9b in Appendix.

4.3 Numerical setup and experimental design

The SP-SAA model and Algorithm 1 are applied to all thirty instances (consisting of five regions and six periods). Algorithm 1 was implemented in Python 3.6 and provided quick, conservative solutions, while the SP-SAA model was implemented in Gurobi 8.1 using multiple threads and provided a benchmark for all spatiotemporal networks. From these thirty SP-SAA test cases, we chose the nine worst-performing instances to test the chance-constrained formulation using Gurobi 8.1. All the tests were performed on a computer with an Intel Core E5-2630 v4 CPU 2.20 GHz and 128 GB of RAM.

For the expectation-based model, we assume that cost function $f(\mathbf{x}) = 0$, because the cost of volunteer vehicles and emergency vehicles utilized is constrained by (8). For the chance-constrained model, we utilize a slightly-adapted formulation from (CC-SAA) to directly examine the tradeoff between cost of volunteer vehicles recruited and probability of full evacuation, given by

$$\min_{x} \quad \sum_{s\in S} \alpha_s x_s \tag{CC-SAA2}$$

$$\text{s.t.} \quad (2)\text{–}(11),$$

$$\sum_{v\in V} \sum_{(i^t,j^{t'})\in A} y_{vi^tj^{t'}\omega} d_{ij} \le D, \quad \omega \in \Omega. \tag{12}$$

Here, the objective is to minimize the cost of volunteer vehicles hired. We move the objective

to minimize expected total distance traveled by all vehicles to constraint (12), putting an upper bound on the distance traveled, D. Otherwise, the constraints of (CC-SAA2) remain the same as (CC-SAA). We slightly amend the out-of-sample testing function from $W(\mathbf{x}, \mathbf{a}(\omega))$ to

$$W'(x, \mathbf{a}(\omega)) = \max_{\mathbf{y}_\omega, \mathbf{z}_\omega, \mathbf{q}_\omega} \sum_{v \in V} \sum_{j^t \in \mathcal{N}_P} q_{vj^t\omega}$$
$$\text{s.t. } (2)\text{–}(9), (12).$$

For each instance tested for each of the three formulations, the five Monte Carlo samples $\Omega_1^{\mathcal{N}'h}, \ldots, \Omega_5^{\mathcal{N}'h}$ are used to obtain 5 candidate solutions $\hat{\mathbf{x}}_1, \ldots, \hat{\mathbf{x}}_5$ with corresponding optimal objective values $w_1, \ldots, w_5$. To perform the SP-SAA tests on regional subnetworks with up to 16 nodes with an hour time limit, we relax the second stage decision variables, $\mathbf{y}_\omega$, $\mathbf{q}_\omega$, and $\mathbf{z}_\omega$, keeping only the first stage decision variables $\mathbf{x}$ integer. Because $w_i \leq u_i$, the optimal solution for the non-relaxed model, the average $\overline{w} = \frac{1}{5}\sum_{i=1}^{5} w_i \leq \frac{1}{5}\sum_{i=1}^{5} u_i = \overline{u}$. Recall that $\mathbb{E}[\overline{u}] \leq u^*$, the optimal value for the problem at hand (Mak et al., 1999), which implies $\overline{w}$ also provides a lower bound for u^*, for $m = 1, \ldots, 5$. An upper bound for u^* is determined by $\hat{u} = \min_{1 \leq m \leq 5} \left\{ \frac{1}{1000} \sum_{\omega \in \Omega_m^{\mathcal{N}'h}} Q(\hat{\mathbf{x}}_m, a(\omega)) \right\}$.

Relaxing variables in the chance-constrained formulation is not as effective, and thus, we solve the full mixed-integer program (CC-SAA2) using Gurobi. For this reason, we decrease the size of $|\Omega_m^{\mathcal{N}'h}|$ from 100 to 25 or 50 for $m = 1, \ldots, 5$ in these tests to decrease computational time. For the largest network, we also set the MIP Focus parameter to 1, to focus on finding feasible solutions. We set the upper bound on distance, $D = 1000$ km, a loose bound for all networks tested.

To compare the computational time and effectiveness of Algorithm 1 directly with the stochastic program, we use the same five samples with 100 scenarios and out-of-sample test with 1000 scenarios. Because these tests perform well, we do not increase the in-sample scenario size, though as noted in Section 3, in-sample scenario size only affects the initialization of the algorithm which for a fixed network is polynomial in $|\Omega_m^{\mathcal{N}'h}|$.

4.4 Benchmark tests

We use Model (SP-SAA) as a benchmark for all thirty instances, and present its in-sample computational time (in second) and solution performance in out-of-sample tests for each of the five regions in Table 3.

For each of the four smaller regions, with pickup locations ranging from 4 to 10, the computational time for each period is less than one hour. For region D, the region with 16 pickup locations, Hours 2, 3, and 5 had samples that timed out, though the mixed-integer program optimality gap is better than .04% in each of these instances. The SAA optimality gap, calculated by taking the difference $\hat{u} - \overline{w}$ and dividing by $|\overline{w}|$, is less than .03 across instances. For all regions and time periods studied, the average percent evacuated across the 1,000 scenarios in the out-of-sample test is at least 97%. In addition, for 21 of the 30 instances, the probability of a complete evacuation is more than .98, according to the out-of-sample empirical distribution. Notably, Region B, with 10 nodes, had a complete evacuation for every out-of-sample scenario in each of the time periods studied. This implies that for 21 of 30 instances of the SP-SAA test, the constraint (CC) holds for

Table 3: In-sample runtime and out-of-sample solution performance of (SP-SAA) for all regions

Region	$\lvert\mathcal{N}_P\rvert$	h	$\mu_h^{\mathcal{N}'}$	In-sample runtime (s)		Out-of-sample % evac.		Prob. of complete evac.
				Mean	Max	Mean	Min	
A	4	1	11.28	0.9	1.11	100	100	1
		2	16.92	1.97	2.39	99.996	95.83	.999
		3	13.63	1.68	1.83	100	100	1
		5	14.57	1.98	2.42	100	100	1
		6	12.22	0.86	1	99.97	88.89	.995
		7	11.75	0.6	0.7	99.99	88.89	.999
B	10	1	34.92	556.77	1049.45	100	100	1
		2	52.38	738.69	2181.39	100	100	1
		3	42.195	140.38	209.04	100	100	1
		5	45.105	645.98	1518.33	100	100	1
		6	37.83	375.62	1171.37	100	100	1
		7	36.375	790.43	1274.7	100	100	1
C	9	1	21.48	22.47	31.98	99.98	95.45	.995
		2	32.22	56.77	157.83	100	96.77	.999
		3	25.955	30.3	54.12	99.56	95.24	.889
		5	27.745	38.97	57	99.99	96.43	.998
		6	23.27	34.15	49.96	97.91	90	.565
		7	22.375	26.9	32.43	98.09	90.48	.605
D	16	1	51.12	1935.6	2854.17	99.3	96.08	67.9
		2	76.68	2424.03*	.02%**	100	100	1
		3	61.77	2705.75*	.04%**	100	100	1
		5	66.03	1977.49*	.03%**	100	100	1
		6	55.38	2423.37	3129.6	99.73	98.08	.835
		7	53.25	1912.97	2511.02	99.17	96.23	.621
E	9	1	21.48	24.53	33.69	99.76	94.74	.947
		2	32.22	60.46	89.65	99.99	96.77	.998
		3	25.955	52.69	58.23	99.99	96	.997
		5	27.745	62.25	101.4	99.93	92.59	.982
		6	23.27	39.01	51.23	99.4	94.44	.86
		7	22.375	35.35	48.82	97.35	89.47	.495

* indicates that the average is taken among all samples that do not time out.
** indicates that the sample times out, and an optimality gap is given.

$\gamma = 1$ and $\epsilon_0 = .02$, using the empirical distribution of the out-of-sample test. In addition, for all but one instance, the constraint (CC) holds for $\gamma = .95$ and $\epsilon_0 = .06$.

Table 4: In-sample runtime and out-of-sample solution performance of (SP-SAA) for Region C in Hour 3.

Second-stage	In-sample runtime (s)		Out-of-sample % evac.		Prob. of complete evac.
	Max	Mean	Min	Mean	
Relaxed	54.12	30.3	95.23	99.56	.889
Integer Program	0.18%*	0.17%*	100	100	1

* indicates that the sample times out, and an optimality gap is given.

Moreover, the effect of relaxing the second-stage problem when finding candidate solutions can be seen in some of the larger instances. For example, using the best candidate solution for Region C at Hour 3, the out-of-sample probability of complete evacuation is .889. At the same time, only 3 of the 10 available cars are hired in the first stage. This candidate solution is clearly suboptimal. Table 4 compares these results with SAA without relaxing the second stage, using the same 5 samples and out-of-sample testing set Ω. Without relaxing the second stage, we find a candidate solution that gives complete evacuation in all out-of-sample scenarios. However, each sample in this trial times out at one hour and we instead present the optimality gaps. Region C only has 9 nodes, and takes at most a minute for each sample with relaxed second-stage variables. Thus, for larger instances, like region D, which already time out for some samples, relaxing the second stage is necessary.

We also explain why some instances perform better in the (SP-SAA) relaxation, in terms of the probability of complete evacuation. Regions C, D, and E all have three periods in which the probability of complete evacuation is less than .95 (see Table 3). In particular, Region C, Hour 6, has out-of-sample probability of full evacuation of .565 and Region E, Hour 7, .495. Each of these regions has 9 pickup locations. On the other hand, Region B has 10 pickup locations, yet has complete evacuation in all out-of-sample tests. One possible explanation is the ratio of $\mu_h^{\mathcal{N}'}$, total expected demand in period h for all locations in network $\mathcal{N}'$ and $t = 4(h-1)+1, \ldots, 4h$, to number of pickup locations. As total expected demand $\mu_h^{\mathcal{N}'}$ increases, number of hired volunteer vehicles increases (see Figure 6 in Section 4.5), and in turn, the set of available volunteer and emergency vehicles tends to be larger. This implies the ratio of available vehicles to pickup locations tends to increase with the ratio of total expected demand $\mu_h^{\mathcal{N}'}$ to number of pickup locations.

The vehicle to pickup location ratio can have an important effect. If a different evacuee arrives at every pickup location during the last epoch, $t = 4h$, and this ratio is less than 1, then a complete evacuation does not happen. Figure 4 illustrates how out-of-sample probability of complete evacuation is steeply concave in the ratio of vehicles to pickup locations. Regions A and B are excluded because the range of the probability is small, between .99 and 1.

The effect of using the rolling horizon approach on the quality of solutions is tested on the smallest network, Region A. As a baseline comparison, we perform SAA with the parameters described in Section 4.2, on each hour individually. To isolate the effect of the rolling horizon approach, in this case, we utilize independent Monte Carlo samples Ω_m^h, $m = 1, \ldots, 5$, for all

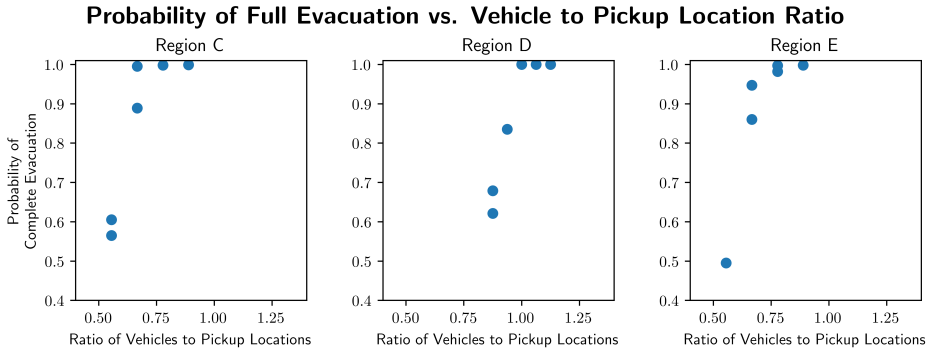

Figure 4: Comparison of out-of-sample probability of complete evacuation and the ratio of available vehicles to number of pickup locations in Regions C, D, E.

seven hours, including both Hour 3 and Hour 4, which have the same demand distribution. Then, we merge the scenarios from Monte Carlo sample $m = 1, \ldots, 5$ for Region A and each hour, Ω_m^h, $h = 1, \ldots, 7$, to create set Ω'_m. For $1 \leq j \leq 1000$, scenario $\omega_j \in \Omega'_m$ is merged as follows: $\omega_j = (\omega_j^1, \ldots, \omega_j^7)$, such that ω_j^h is the j^{th} scenario from sample Ω_m^h. We perform SAA on on set Ω'_m with $T = 28$.

Table 5: Evacuees served by rolling-horizon approach compared with SAA for Region A.

Approach	In-sample runtime (s)		Out-of-sample % evac. (minimum)	Prob of complete evac.
	Max	Mean		
Rolling Horizon	11.70	10.22	98.02	.993
$T = 28$ (SAA)	N/A**	2160.48*	98.11	.994

*: the average is taken among all samples that do not time out; **: the sample times out.

Note in Table 5, the evacuation rates are comparable in the rolling horizon and SAA approaches (with $T = 28$). Across 1000 scenarios in the out-of-sample test, the minimum percentage evacuated is 98.02% and 98.11% for the rolling horizon and SAA approaches, respectively. The distance traveled and number of volunteer cars hired, described in Table 6, are much higher, however.

Table 6: Travel distance and hired cars by rolling-horizon approach compared with SAA for Region A.

Approach	In-sample runtime (s)		Distance traveled		# of hired cars from S
	Max	Mean	Max	Mean	
Rolling Horizon	11.7	10.22	918.9	720.36	19
$T = 28$ (SAA)	N/A**	2160.48*	792.7	329.14	9

*: the average is taken among all samples that do not time out; **: the sample times out.

Figure 5 depicts the effect of each individual volunteer vehicle and emergency vehicle on the ability to serve evacuees for Region D at Hour 2. This instance involves the largest network with the highest expected demand over the period, for all pickup nodes. All scenarios are completely evacuated in the out-of-sample tests for a candidate solution with 9 volunteer cars dispersed amongst 6 pickup locations. We randomly remove a car one at a time from these 9 volunteer cars to create candidate solutions with 3, 4, 5, 6, 7, and 8 volunteer cars. For the same instance, we fix the 9

volunteer car solution, and reduce the emergency cars available to 5, 6, 7, and 8. The average percent evacuated and out-of-sample probability of full evacuation are compared in Figure 5. As can be seen in the left figure, average percent evacuated is concave in both volunteer and emergency cars, with decreasing emergency cars and their greater capacity having a larger effect on average percent evacuated. In the right figure, we can see that out-of-sample probability of complete evacuation as a function of number of vehicles has an S-shaped curve for both emergency and volunteer vehicles.

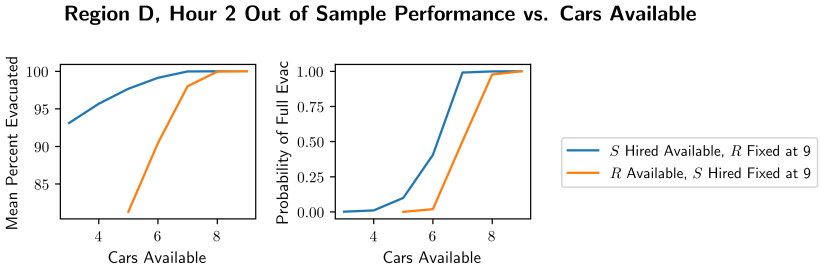

Figure 5: Comparison of out-of-sample mean percent evacuated and probability of full evacuation for different sizes of hired cars $\boldsymbol{S}$ and emergency cars $\boldsymbol{R}$ available for Region D, Hour 2.

4.5 Chance-constrained formulation and Algorithm 1 tests

Using (SP-SAA) as a benchmark, we perform a number of tests with the chance-constrained formulation and Algorithm 1. Because the main advantage of (CC-SAA2) is ensuring reliable solutions, and (SP-SAA) performs very reliably in 21 of 30 test instances, producing solutions that ensure full evacuation with probability at least .98, we only perform (CC-SAA2) on the nine worst-performing instances. These test cases ensure full evacuation with probability less than .95. Correspondingly, the goal of the chance-constrained formulation tests is to produce solutions that satisfy the probabilistic constraint (CC) with $\gamma = 1$ and $\epsilon_0 = .05$, with respect to the empirical out-of-sample probability distribution.

On the other hand, the key advantage of Algorithm 1 is computational speed. The thirty (SP-SAA) benchmarks range in mean runtime from .6 to 2705.75 seconds, and some samples time out. For this reason, we are interested in comparing performance and computational time for all thirty instances.

It is important to keep in mind that the objectives of (SP-SAA) and (CC-SAA2) differ. While the objective of (SP-SAA) is to hire a set of volunteer vehicles that maximizes expected demand served and minimizes expected distance traveled, (CC-SAA2) aims to minimize the *cost* of hired volunteer vehicles, subject to a probabilistic constraint, which ensures complete evacuation with a particular probability, and feasibility constraints, which include an upper bound on distance traveled for each scenario. Thus, by design, (SP-SAA) tends to favor smaller distance traveled and (CC-SAA2) tends to favor smaller sets of volunteer cars hired.

Both formulations utilize the sample average approximation technique, and in both cases, we uti-

lize samples $\Omega_1^{\mathcal{N}'h}, \ldots, \Omega_5^{\mathcal{N}'h}$ to find candidate solutions $\hat{\mathbf{x}}_1, \ldots, \hat{\mathbf{x}}_5$. We then perform out-of-sample tests with $\Omega^{\mathcal{N}'h}$ to find the best candidate solution. How we rank these candidate solutions depends on the formulation, however. Corresponding to the objectives of (SP-SAA) and (CC-SAA2), the best candidate solution is defined as follows:

$$\mathbf{x}^* = \begin{cases} \underset{\hat{\mathbf{x}}_m : m=1,\ldots,5}{\operatorname{argmin}} \left\{ \frac{1}{1000} \sum_{\omega \in \Omega_m^{\mathcal{N}'h}} Q(\hat{\mathbf{x}}_m, \mathbf{a}(\omega)) \right\}, & \text{for (SP-SAA)}, \\ \underset{\hat{\mathbf{x}}_m : m=1,\ldots,5}{\operatorname{argmin}} \left\{ \frac{1}{1000} \sum_{\omega \in \Omega_m^{\mathcal{N}'h}} \boldsymbol{\alpha}^\mathsf{T} \hat{\mathbf{x}}_m : \mathbb{P}_{\Omega_m^{\mathcal{N}'h}} \big(W'(\hat{\mathbf{x}}_m, \mathbf{a}(\omega)) = \mathbf{a}(\omega) \big) > .95 \right\}, & \text{for (CC-SAA2)}, \end{cases}$$

where $\mathbb{P}_{\Omega_m^{\mathcal{N}'h}}$ represents the probability with respect to the out-of-sample distribution and $\boldsymbol{\alpha} = [\alpha_s : s \in S]^\mathsf{T}$. Note that Algorithm 1 provides a quick, greedy solution, without regard to a particular cost objective. Thus, it would be reasonable to compare its performance to either (SP-SAA) or (CC-SAA2) directly, using the same samples $\Omega_1^{\mathcal{N}'h}, \ldots, \Omega_5^{\mathcal{N}'h}$ to produce candidate solutions, and then ranking those candidate solutions using either metric for $\mathbf{x}^*$. Because (SP-SAA) is the benchmark we use, and for which we performe tests for all thirty instances, we use the (SP-SAA) metric to determine $\mathbf{x}^*$ for the tests of Algorithm 1.

To decrease computational time, for the chance-constrained formulation, we relax a few parameters. For Region C and E, containing 9 pickup locations each, we relax $\epsilon = .05$ to .1. We utilize the first 50 scenarios in each of the five Monte Carlo samples generated for the (SP-SAA) tests. For Region D, with 16 pickup locations, we let ϵ be quite large, .7, and utilize the first 25 scenarios. Because we require $\gamma = 1$, the intuition is that a solution that satisfies complete evacuation for 90% (or 30%, respectively) of scenarios would likely do well in many scenarios. Ultimately, using these parameters, we are able to ensure complete evacuation with probability of at least .965 for all nine instances.

Table 7 compares the in-sample runtime and out-of-sample successful evacuation rates given by optimal solutions of the stochastic program, chance-constrained formulation, and Algorithm 1. For all nine instances, (CC-SAA2) and Algorithm 1 ensure full evacuation with out-of-sample probability greater than .965. Because it is not possible to relax any integer variables in the chance-constrained formulation, it takes the longest to solve, timing out in at least one sample for all but one instance – Region C, Hour 7. Algorithm 1, on the other hand, has a mean runtime of less than a tenth of a second for all nine test cases.

Table 8 compares the costs associated with the solutions of the nine instances given by different methods. Algorithm 1 requires more vehicles than the chance-constrained formulation, which in turn requires more vehicles than the stochastic program. As noted earlier, changing the metric for the heuristic solution $\mathbf{x}^*$ could potentially decrease the number of vehicles hired, if this objective is of interest to decision makers.

The mean distance traveled for the solution of Algorithm 1 is less than the mean distance traveled for the (SP-SAA) solution in 8 of 9 instances, and within a kilometer for the last instance. This makes sense, as there are more cars in Algorithm 1's solutions, meaning that vehicles are more likely able to stay in their origin zone. We find that indeed for all 9 instances, the average

Table 7: In-sample runtime and out-of-sample evacuation performance by SP-SAA, CC-SAA2, and Algorithm 1.

$\mathcal{N}'$	h	In-sample runtime (s) (mean)			Prob. of complete evac.		
		SP-SAA	CC-SAA	Algorithm 1	SP-SAA	CC-SAA2	Algorithm 1
C	3	30.3	76.67%*	***	0.889	1	1
C	6	34.15	1823.93**	***	0.565	0.965	1
C	7	26.9	2366.51	***	0.605	0.981	1
D	1	1935.6	100%*†	***	0.679	1	1
D	6	2423.37	100%*†	***	0.835	1	1
D	7	1912.97	100%*†	***	0.621	1	1
E	1	24.53	2355.04**	***	0.947	1	1
E	6	39.01	2651.77**	***	0.86	1	1
E	7	35.35	2418.25**	.01	0.495	1	1

*: optimality gap; **: average taken among samples that do not time out;
***:<.01 seconds; †: MIP finds feasible solutions.

Table 8: Out-of-sample travel distance and # of cars hired by SP-SAA, CC-SAA2, and Algorithm 1.

$\mathcal{N}'$	h	# of cars hired			Distance traveled (km) (mean)		
		SP-SAA	CC-SAA	Algorithm 1	SP-SAA	CC-SAA	Algorithm 1
C	3	3	4	6	152.6	245.15	142.83
C	6	2	3	4	147.09	196.95	141.12
C	7	2	3	4	142.79	193.21	137.30
D	1	8	10	11	289.36	516.53	282.89
D	6	9	11	13	304.56	533.21	288.00
D	7	8	11	13	293.77	529.75	274.52
E	1	4	5	5	152.8	242.88	139.92
E	6	3	4	4	150.27	247.8	150.88
E	7	2	4	4	150.62	239.93	145.90

number of cars that leave their origin zone increases, ranging from a 2% increase for Region E, Hour 7 to a 23% increase from 3.73 to 4.59 average emergency and volunteer vehicles leaving their origin zone for Region E, Hour 1. The median increase is 5%. In addition, (CC-SAA2) has much larger mean distance traveled values, which makes sense, as the upper bound on distance traveled for each scenario is loose, with $D = 1000$.

A comparison of all thirty instances of (SP-SAA) and Algorithm 1 can be seen in Figure 6. For larger values of total expected demand, $\mu_h^{\mathcal{N}'}$, the (SP-SAA) in-sample runtime tends to be higher, while Algorithm 1's runtime remains steady, in the first graph. On the other hand, the number of hired volunteer cars tends to be larger for both for larger values of $\mu_h^{\mathcal{N}'}$ in the second graph. In general, Algorithm 1's solutions tend to have a larger set of hired vehicles than (SP-SAA)'s solutions. In the third graph, we compare the out-of-sample probability of full evacuation, which is consistently 1 for Algorithm 1, while lower in some cases for (SP-SAA).

Finally, we compare the in-sample runtime and out-of-sample detailed solution performance given by (SP-SAA) and Algorithm 1 for all the regions in Table 9.

5 Conclusion

In this paper, we examined a resource planning for ridesharing-based evacuation problem. We formulated the problem as a two-stage stochastic program and a chance-constrained formulation,

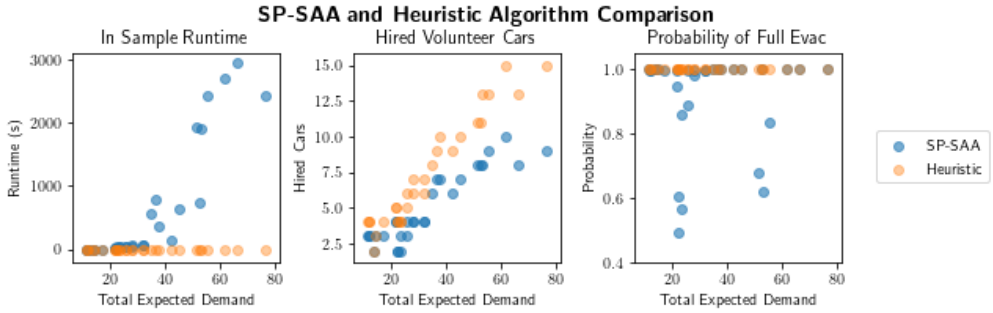

Figure 6: Comparison of in-sample runtime, number of hired cars and probability of full evacuation for the optimal candidate solutions given by SP-SAA and Algorithm 1.

Table 9: In-sample runtime and out-of-sample solution performance of (SP-SAA) and Algorithm 1 for all regions

$\mathcal{N}'$	h	In-sample runtime (s)				Prob. of Complete Evac.		# of cars hired	
		SP-SAA		Algorithm 1		SP-SAA	Algorithm 1	SP-SAA	Algorithm 1
		Mean	Max	Mean	Max				
A	1	0.9	1.11	***	***	1	1	3	4
	2	1.97	2.39	***	***	0.999	1	3	4
	3	1.68	1.83	***	***	1	1	2	2
	5	1.98	2.42	***	***	1	1	3	3
	6	0.86	1	***	***	0.995	1	3	4
	7	0.6	0.7	***	***	0.999	1	3	4
B	1	556.77	1049.45	***	***	1	1	6	8
	2	738.69	2181.39	***	***	1	1	8	11
	3	140.38	209.04	***	***	1	1	6	9
	5	645.98	1518.33	***	***	1	1	7	10
	6	375.62	1171.37	***	***	1	1	7	10
	7	790.43	1274.7	***	0.01	1	1	7	9
C	1	22.47	31.98	***	***	0.995	1	4	5
	2	56.77	157.83	***	***	0.999	1	4	7
	3	30.3	54.12	***	***	0.889	1	3	6
	5	38.97	57	***	***	0.998	1	4	7
	6	34.15	49.96	***	***	0.565	1	2	4
	7	26.9	32.43	***	***	0.605	1	2	4
D	1	1935.6	2854.17	***	***	0.679	1	8	11
	2	2424.03*	.02%**	***	0.01	1	1	9	15
	3	2705.75*	.04%**	***	0.01	1	1	10	15
	5	1977.49*	.03%**	0.01	0.01	1	1	8	13
	6	2423.37	3129.6	***	0.01	0.835	1	9	13
	7	1912.97	2511.02	***	***	0.621	1	8	13
E	1	24.53	33.69	***	***	0.947	1	4	5
	2	60.46	89.65	***	0.01	0.998	1	4	6
	3	52.69	58.23	***	***	0.997	1	4	5
	5	62.25	101.4	***	***	0.982	1	4	6
	6	39.01	51.23	***	***	0.86	1	3	4
	7	35.35	48.82	.01	.01	0.495	1	2	4

*: the average is taken among all samples that do not time out; **: optimality gap; ***: <.01 seconds.

and developed a quick heuristic. We tested our models and heuristic algorithm (Algorithm 1) using a variety of instances, with different geographical sizes and varying population density, based on the Charleston area, which experienced a mandatory hurricane evacuation in September 2018.

The stochastic program, which acted as a benchmark for all models, had an average evacuation rate of at least 97% for all instances. (SP-SAA) provided fairly reliable solutions as well, with 21 of 30 instances ensuring full evacuation with probability at least .98 with respect to the out-of-sample distribution. For the other nine instances, (CC-SAA2) provided reliable solutions, ensuring complete evacuation with probability at least .965. The (CC-SAA2) solutions required at least one more vehicle than the corresponding (SP-SAA) solutions, and had larger mean total distance traveled.

Algorithm 1 was able to find reliable solutions in less than a tenth of a second for all samples and instances tested. For all instances, Algorithm 1's solutions ensured complete evacuation with probability 1. The heuristic solutions generally required more cars than the (SP-SAA) solution, and for the instances in which (CC-SAA2) was tested, the heuristic solutions required more cars than those solutions as well.

The SP-SAA tests showed an increasing concave relationship between the probability of complete evacuation and the available vehicle to pickup location ratio, $\frac{1^{\mathsf{T}}\mathbf{x}^*+|R|}{|\mathcal{N}_P|}$. In addition, the number of available vehicles tended to increase with the total expected demand of a particular spatiotemporal instance. Thus, the total expected demand to pickup location ratio, a measure of population density, is a characteristic of the spatiotemporal network that is related to the reliability of (SP-SAA). Spatiotemporal networks with high population density may be better candidates for (SP-SAA), while spatiotemporal networks with lower population density may be better candidates for (CC-SAA2) or Algorithm 1. Overall, Algorithm 1 can provide quick, reliable solutions across a variety of instances.

In this work, we considered heterogeneous hiring decisions, routing decisions, and loading decisions, under uncertainty in spatiotemporal demand. Our focus is on serving carless elderly populations, individuals with disabilities, and others who require specialized assistance, to complement the work that has been done on larger-scale transit-dependent evacuation. One potential future research question is how to best integrate large-scale transit and shared mobility in a comprehensive evacuation plan, identifying which populations to assign to which transportation mode and how to time the evacuations, taking into account changing density of traffic and different congestive factors of buses versus personal vehicles.

Acknowledgements

The authors are grateful for the partial support from the U.S. National Science Foundation grant #1727618 and U.S. Department of Engineering (DoE) grant #DE-SC0018018.

References

Bayram, V. (2016). Optimization models for large scale network evacuation planning and management: A literature review. *Surveys in Operations Research and Management Science*, 21(2):63–84.

Ben-Tal, A., Do Chung, B., Mandala, S. R., and Yao, T. (2011). Robust optimization for emergency logistics planning: Risk mitigation in humanitarian relief supply chains. *Transportation Research Part B: Methodological*, 45(8):1177–1189.

Birge, J. R. and Louveaux, F. (2011). *Introduction to Stochastic Programming*. Springer Science & Business Media.

Bish, D. R. (2011). Planning for a bus-based evacuation. *OR Spectrum*, 33(3):629–654.

Caunhye, A. M., Nie, X., and Pokharel, S. (2012). Optimization models in emergency logistics: A literature review. *Socio-Economic Planning Sciences*, 46(1):4–13.

Charnes, A. and Cooper, W. W. (1959). Chance-constrained programming. *Management Science*, 6(1):73–79.

Charnes, A. and Cooper, W. W. (1962). Chance constraints and normal deviates. *Journal of the American Statistical Association*, 57(297):134–148.

Cordeau, J.-F. and Laporte, G. (2007). The dial-a-ride problem: Models and algorithms. *Annals of Operations Research*, 153(1):29–46.

FEMA (2006). *Multi-hazard loss estimation methodology: Earthquake model, HAZUS-MH MR2 User Manual*. Department of Homeland Security, FEMA, Washington, DC.

Gan, H.-S., Richter, K.-F., Shi, M., and Winter, S. (2016). Integration of simulation and optimization for evacuation planning. *Simulation Modelling Practice and Theory*, 67:59–73.

Goerigk, M., Deghdak, K., and T'Kindt, V. (2015). A two-stage robustness approach to evacuation planning with buses. *Transportation Research Part B: Methodological*, 78:66–82.

Kleywegt, A. J., Shapiro, A., and Homem-de Mello, T. (2002). The sample average approximation method for stochastic discrete optimization. *SIAM Journal on Optimization*, 12(2):479–502.

Kulshrestha, A., Lou, Y., and Yin, Y. (2014). Pick-up locations and bus allocation for transit-based evacuation planning with demand uncertainty. *Journal of Advanced Transportation*, 48(7):721–733.

Legg, M. R., Nozick, L. K., and Davidson, R. A. (2010). Optimizing the selection of hazard-consistent probabilistic scenarios for long-term regional hurricane loss estimation. *Structural Safety*, 32(1):90–100.

Li, A. C., Nozick, L., Xu, N., and Davidson, R. (2012). Shelter location and transportation planning under hurricane conditions. *Transportation Research Part E: Logistics and Transportation Review*, 48(4):715–729.

Li, Y. (2017). *Robust Vehicle Routing in Disaster Relief and Ride-Sharing: Models and Algorithms*. PhD thesis, Binghamton University–SUNY, Binghamton, NY.

Lim, G. J., Rungta, M., and Davishan, A. (2019). A robust chance constraint programming approach for evacuation planning under uncertain demand distribution. *IISE Transactions*, 51(6):589–604.

Litman, T. (2006). Lessons from Katrina and Rita: What major disasters can teach transportation planners. *Journal of Transportation Engineering*, 132(1):11–18.

Liu, C., Aleman, D. M., and Beck, J. C. (2018). Modelling and solving the senior transportation problem. In *International Conference on the Integration of Constraint Programming, Artificial Intelligence, and Operations Research*, pages 412–428. Springer.

Lu, W., Liu, L., Wang, F., Zhou, X., and Hu, G. (2020). Two-phase optimization model for ride-sharing with transfers in short-notice evacuations. *Transportation Research Part C: Emerging Technologies*, 114:272–296.

Luedtke, J. and Ahmed, S. (2008). A sample approximation approach for optimization with probabilistic constraints. *SIAM Journal on Optimization*, 19(2):674–699.

Mak, W.-K., Morton, D. P., and Wood, R. K. (1999). Monte Carlo bounding techniques for determining solution quality in stochastic programs. *Operations Research Letters*, 24(1-2):47–56.

Manno, A. (2018). Evacuations with I-26 lane reversals for Charleston and most of S.C. coast ordered for Tuesday at noon. Charleston City Paper, `https://www.charlestoncitypaper.com/TheBattery/archives/2018/09/10/evacuations-with-i-26-lane-reversals-for-charleston-and-entire-sc-coast-ordered-for-tuesday-at-noon`.

Naoum-Sawaya, J. and Yu, J. Y. (2017). Ridesharing for emergency evacuation. *INFOR: Information Systems and Operational Research*, 55(4):339–358.

Radwan, A., Hobeika, A., and Sivasailam, D. (1985). Computer simulation model for rural network evacuation under natural disasters. *ITE Journal*, 55(9):25–30.

Renne, J. L., Sanchez, T. W., and Litman, T. (2011). Carless and special needs evacuation planning: A literature review. *Journal of Planning Literature*, 26(4):420–431.

Saadatseresht, M., Mansourian, A., and Taleai, M. (2009). Evacuation planning using multiobjective evolutionary optimization approach. *European Journal of Operational Research*, 198(1):305–314.

Savelsbergh, M. W. and Sol, M. (1995). The general pickup and delivery problem. *Transportation Science*, 29(1):17–29.

Shapiro, A., Dentcheva, D., and Ruszczyński, A. (2014). *Lectures on Stochastic Programming: Modeling and Theory*. SIAM.

South Carolina Department of Transportation (2018). Traffic counts. `https://www.scdot.org/travel/travel-trafficdata.aspx`.

Tanaka, A., Hata, N., Tateiwa, N., and Fujisawa, K. (2017). Practical approach to evacuation planning via network flow and deep learning. In *2017 IEEE International Conference on Big Data (Big Data)*, pages 3368–3377. IEEE.

Toth, P. and Vigo, D. (2002). *The Vehicle Routing Problem*. SIAM.

Tweedie, S. W., Rowland, J. R., Walsh, S. J., Rhoten, R. P., and Hagle, P. I. (1986). A methodology for estimating emergency evacuation times. *The Social Science Journal*, 23(2):189–204.

United States Census Bureau (2018a). 2018 ACS 5-Year Estimates Data Profiles: ACS Demographic and Housing Estimates. `https://data.census.gov/cedsci/`.

United States Census Bureau (2018b). 2018 ACS 5-Year Estimates Subject Profiles: Median Income in the Past 12 Months (in 2018 Inflation-Adjusted Dollars). `https://data.census.gov/cedsci/`.

Urbina, E. and Wolshon, B. (2003). National review of hurricane evacuation plans and policies: a comparison and contrast of state practices. *Transportation Research Part A: Policy and Practice*, 37(3):257–275.

Wang, L. (2020). A two-stage stochastic programming framework for evacuation planning in disaster responses. *Computers & Industrial Engineering*, page 106458.

Wang, L., Yang, L., Gao, Z., Li, S., and Zhou, X. (2016). Evacuation planning for disaster responses: A stochastic programming framework. *Transportation Research Part C: Emerging Technologies*, 69:150–172.

Wong, R. T. (2008). Vehicle routing for small package delivery and pickup services. In *The Vehicle Routing Problem: Latest Advances and New Challenges*, pages 475–485. Springer.

Yu, M. and Shen, S. (2020). An integrated car-and-ride sharing system for mobilizing heterogeneous travelers with application in underserved communities. *IISE Transactions*, 52(2):151–165.

Yusoff, M., Ariffin, J., and Mohamed, A. (2008). Optimization approaches for macroscopic emergency evacuation planning: a survey. In *2008 International Symposium on Information Technology*, volume 3, pages 1–7. IEEE.

Appendix: Expected Demand and Volunteer Distributions

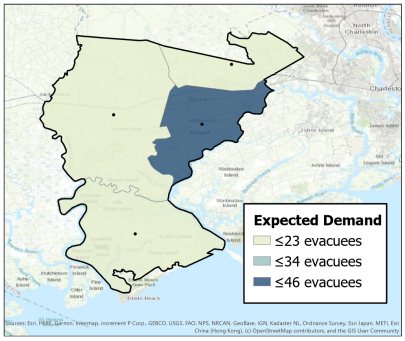

(a) Region A – Expected Demand

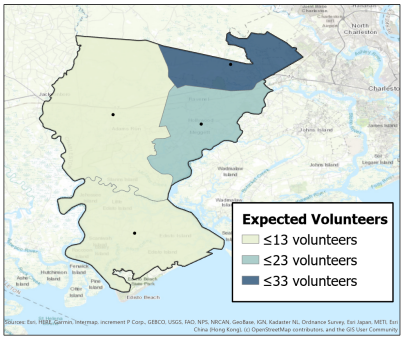

(b) Region A – Expected Volunteers

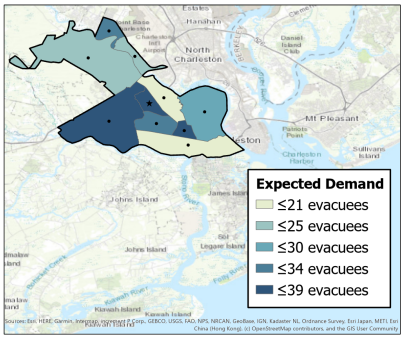

(c) Region B – Expected Demand

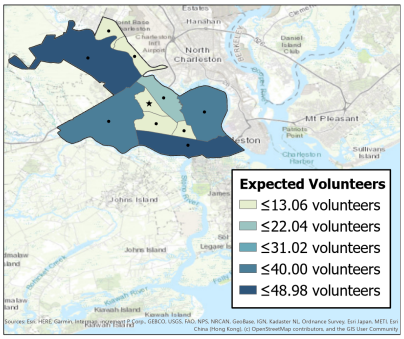

(d) Region B – Expected Volunteers

Figure 7: Spatial distributions of expected evacuation demand and number of volunteers in Regions A and B.

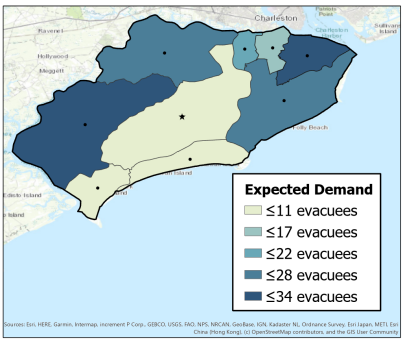

(a) Region C – Expected Demand

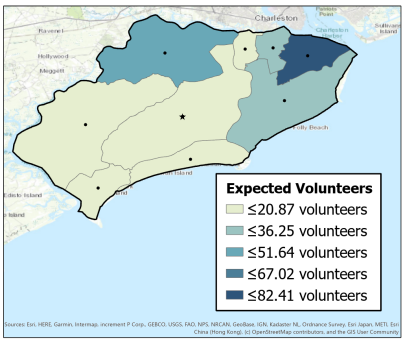

(b) Region C – Expected Volunteers

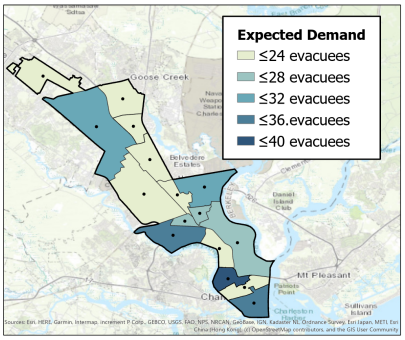

(c) Region D – Expected Demand

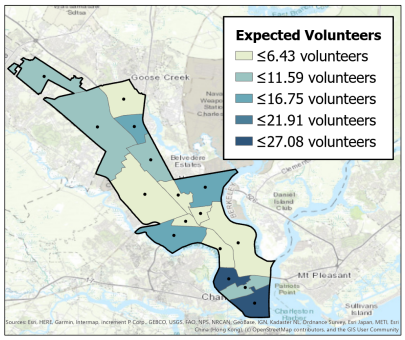

(d) Region D – Expected Volunteers

Figure 8: Spatial distributions of expected evacuation demand and number of volunteers in Regions C and D.

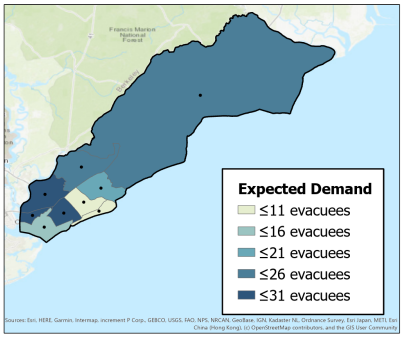

(a) Region E – Expected Demand

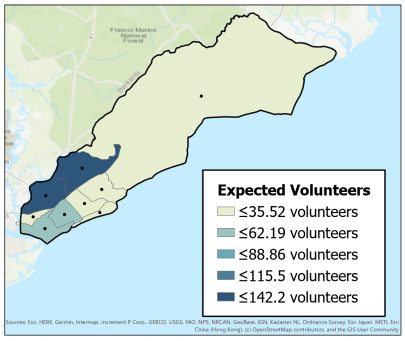

(b) Region E – Expected Volunteers

Figure 9: Spatial distributions of expected evacuation demand and number of volunteers in Region E.